

## **Can we predict the existence of extrarenal feeders to renal angiomyolipomas?**

### **Abstract**

#### **Objectives**

To identify factors predicting the presence of extrarenal feeders to renal angiomyolipomas (AMLs).

#### **Methods**

This is a retrospective study of 44 patients with 58 renal AMLs embolized in our department. Arteriography obtained during embolization and CTA obtained before and after embolization were reviewed to characterize AMLs with and without extrarenal feeders. Tumor characteristics were compared between the two groups. Simple logistic regression and ROC curve analysis were performed.  $P < 0.05$  was considered to be statistically significant.

#### **Results**

Of the 58 AMLs reviewed, 29% had extrarenal arteries and 71% did not. AMLs with extrarenal feeders were significantly larger than those without, in terms of volume (median, 368 mL versus 109 mL,  $p < 0.0002$ ) and largest diameter (mean, 12.0 cm versus 7.7 cm,  $p < 0.0001$ ). Patient age, presence of tuberous sclerosis complex or sporadic lymphangioleiomyomatosis, and tumor location did not differ between the groups. Largest diameter and volume had similar predictive values for the presence of extrarenal feeders (AUC, 0.83 versus 0.82,  $p = 0.673$ ). Extrarenal feeders were present in 0%, 21%, and 79% of the AMLs  $\leq 6.5$  cm, AMLs 6.6–10.5 cm, and AMLs  $>10.5$  cm, respectively.

## **Conclusions**

AML size correlates with the presence of extrarenal feeders, with largest diameter and volume being significant predictors. AMLs >10.5 cm had a high chance of extrarenal feeders, making it mandatory to search for feeders to them in order to avoid incomplete embolization; AMLs ≤6.5 cm did not have extrarenal feeders, making a search for them unnecessary in these cases.

## **Key words**

Angiomyolipoma; Arteries; Angiography; Endovascular Procedures; Kidney Neoplasms

## **Key points**

1. The presence of extrarenal feeders to renal angiomyolipoma is associated with tumor size, but not with patient age, concomitant disease, or tumor location.
2. Largest diameter and volume predict the presence of extrarenal feeders to AML, with similar predictive values.
3. AMLs >10.5 cm have a high chance (79%) of extrarenal feeders, making it mandatory to search for feeders to them in order to avoid incomplete embolization; AMLs ≤6.5 cm do not have extrarenal feeders, making a search for them unnecessary in these cases.

## **Abbreviations and acronyms**

AB	Aortic branches
AML	Angiomyolipoma
MPR	Multiphase reconstruction

NSS	Nephron-sparing surgery
RB	Renal arterial branches
sLAM	Sporadic lymphangioliomyomatosis
TAE	Transcatheter arterial embolization
TSC	Tuberous sclerosis complex

## **Introduction**

Angiomyolipoma (AML), the most common renal mesenchymal neoplasm, with a frequency of 1%–3% in the general population, originates from perivascular epithelioid cells and consists of muscle, blood vessels, and fat [1]. Most AMLs (95%) can be specifically diagnosed on the basis of macroscopic fat detected on computed tomography (CT) or magnetic resonance imaging (MRI) [2]. Renal AMLs can occur sporadically or associated with tuberous sclerosis complex (TSC) or, more rarely, sporadic lymphangioliomyomatosis (sLAM) [3]. TSC is an autosomal dominant genetic syndrome with a frequency of 1/6000–1/12000 [4, 5], and 40%–80% of TSC patients have renal AMLs, which are frequently multiple and bilateral [6].

Lymphangioliomyomatosis is a rare disease (5–10/million women) and manifests as lung cysts and lymphatic abnormalities [7, 8]. In addition to sporadic cases, it can be associated with TSC. Up to 50% of patients with sLAM have renal AMLs [7, 9].

The classic triad of AML includes flank pain, a palpable tender mass, and gross hematuria [10]. The tumors have the potential to grow substantially and may cause a variety of problems, including mass effect, renal dysfunction, venous thrombosis, and bleeding [11].

For asymptomatic cases, active surveillance is the most common management choice. Tumor size >4 cm or the presence of aneurysm >5 mm, which are

hemorrhagic risk factors, or the presence of patient symptoms are indicators for treatment [12-14]. Renal AML treatment goals focus on preserving renal function while ameliorating any symptoms and risks of renal hemorrhage, which can be accomplished by nephron-sparing surgery (NSS) and selective transcatheter arterial embolization (TAE) [15, 16]. In the setting of acute bleeding, NSS is difficult and can lead to hemostasis nephrectomy; therefore, there is a consensus to recommend TAE as a first-line treatment for acute cases [17]. Furthermore, selective TAE can still be used in cases with very large, central, or endophytic renal AML that precludes NSS [18]. In addition, TAE is a minimally invasive procedure and has a shorter recovery time and less frequent procedure-associated complications than NSS. However, when using selective TAE to manage renal AML, tumor re-growth and re-bleeding after embolization remain a concern [19].

The arteries feeding the target renal AML should be carefully identified by using CT angiography (CTA) or conventional arterial angiography before or during TAE because their identification is closely associated with the success of TAE [11, 20, 21]. In addition to intrarenal arterial branches from segmental arteries, extrarenal arteries may also supply renal AMLs. Existing but unidentified extrarenal feeders can cause incomplete embolization of the target AML, which in turn can cause a recurrence after TAE. Therefore, knowledge of the extrarenal feeders of renal AMLs is necessary. The goal of this study was to identify predictors of the presence of extrarenal feeders to renal AMLs.

## **Materials and methods**

### **Subjects**

This retrospective study was approved by the institutional review board, and the requirement for informed consent was waived. All consecutive patients (n = 68) who underwent selective TAEs of renal AMLs (n = 92) between July 2010 and August 2016 in the authors' department were retrieved from the radiological reporting system. A total of 58 AMLs in 44 patients were ultimately included in this study on the basis of the following criteria: 1) Pre-embolization CT scans containing abdominal CTA were performed in our department; 2) no previous therapy for renal AML was performed before our TAE; and 3) no prior or active hemorrhage from renal AML was present at the time of TAE. Of the 44 patients (mean age, 40 years; range of age, 17-66 years; 43 women and 1 man), 18 (41%) had TSC, 17 (39%) had sLAM, and 9 (20%) had no concomitant disease. The diagnosis of TSC was performed according to the 2012 updated diagnostic criteria for TSC [22] and the diagnosis of sLAM was made according to the European Respiratory Society criteria [23].

### **CT examination and TAE**

For each patient, a pre-embolization CT examination was performed on a 64-slice helical CT scanner (Aquilion 64, Canon Medical Systems; detector design, 64 × 0.5 mm) or a 320-slice helical CT scanner (Aquilion One Vision Edition, Canon Medical Systems; detector design, 320 × 0.5 mm) by using the following established protocol. First, before contrast injection, a non-contrast CT scan was performed from the diaphragm to the symphysis pubis to detect renal AMLs. Then, a four-phase dynamic contrast-enhanced CT scan was performed from the diaphragm to the iliac bifurcation or to the lower level of the kidney (in cases with huge AMLs that reached the pelvic cavity). With volumetric datasets obtained during the arterial phase, CTA images were obtained, including coronal multiplanar reconstruction (MPR) (slice thickness, 3

mm) and 3-dimensional (3-D) CTA images, which were generated by using the imaging software of Ziostation 2 (Ziosoft Inc.).

Prior to TAE, CTA images were reviewed to determine the location and number of renal arteries, and to identify potential non-renal feeding arteries originating from the aortic branches (AB). Since CTA was used to guide the embolization procedure, abdominal aortography was not routinely performed. After the main trunk of the renal artery or the aberrant renal artery was catheterized, renal arteriography was performed following the administration of contrast agent (PRO SCOPE 300 Syringe, Alfresa) at a concentration of 300 mg I/mL, a speed of 2.0–3.0 mL/s, and a volume of 8–12 mL. On renal arteriography, feeding arteries derived from the renal artery or its branches were identified. Subsequently, intermittent confirmatory angiography followed by superselective embolization was performed. Embolic agents used for occlusion were 1-mm multiporous gelatin sponge particles (Gelpart; Nippon Kayaku Co. Ltd.) alone or combined with micro-coils (Tornado/Hilal [Cook Medical LLC]; Target/GDC [Stryker Corp.]; Trufill DCS Orbit [Codman & Shurtleff Inc.]). After embolization, control renal arteriography was performed.

About 1 month after embolization, non-contrast and contrast-enhanced CT scans were performed using the same protocol as that used for the pre-embolization CT examination, and coronal MPRs (slice thickness, 3 mm) were generated.

### **Diagnosis and location of renal AMLs**

On pre-embolization CT images, each tumor contained macroscopic fat, which was consistent with the diagnosis of AML; all tumors were categorized according to location as upper pole, middle portion, or lower pole.

### **Determination of renal AMLs with extrarenal feeders**

For each tumor, pre-embolization CTA images were reviewed to identify extrarenal feeders originating from the AB, such as the middle adrenal artery, the ureteral artery (Figure 1), or the inferior mesenteric artery (Figure 1), which were termed AB-origin extrarenal feeders. For each tumor, renal arteriography obtained during TAE was retrospectively reviewed to determine extrarenal feeders originating from the renal arterial branches (RB), such as the renal capsular artery (Figure 2), the inferior adrenal artery, and the gonadal artery, but which did not supply the renal parenchyma. Those feeders were termed RB-origin extrarenal feeders.

In total, six AB-origin extrarenal feeders and 17 RB-origin extrarenal feeders were detected that fed a total of 17 renal AMLs. At the time of embolization, all 23 of the extrarenal feeders (17 of RB origin and 6 of AB origin) were confirmed (Figure 1) and no other extrarenal feeders were found. None of the 17 tumors had other new or recurrent extrarenal feeders identified retrospectively on review of the post-TAE CTA images. In the present study, the 17 tumors were determined to be renal AMLs with extrarenal feeders.

### **Determination of renal AMLs without extrarenal feeders**

A total of 41 tumors were detected to have no RB-origin extrarenal feeders on renal arteriography and no AB-origin extrarenal feeders on pre-embolization CTA images. For each of these 41 tumors, no extrarenal feeders had been found at the time of embolization, and the absence of extrarenal feeders was confirmed by retrospectively reviewing the post-TAE CTA. Therefore, the 41 tumors were determined to be renal AMLs without extrarenal feeders.

The determination of renal AMLs with or without extrarenal feeders was performed by two radiologists (X.Z. and R.K.) who reviewed all the images together to reach a consensus.

### **Volume and largest diameter of AMLs**

Pre-embolization axial enhanced CT images of each tumor (slice thickness, 5 mm) were loaded into Synapse Vincent software (Fujifilm). Two radiologists (X.Z. and R.K.) reviewed the images together to reach a consensus on delineating the tumor margins. A reconstruction of the tumor in the 3-D plane was automatically obtained and the volume was calculated by the software. Pre-embolization axial and coronal CT images were reviewed to obtain the largest diameter of the target AML, which was defined as the largest measurement of the tumor in either plane.

### **Statistical analyses**

Continuous variables are presented as the mean ( $\pm$  standard deviation) if the data were normally distributed and as the median (interquartile range) if they were not; categorical variables are presented as percentages and frequencies. For comparisons between AMLs with extrarenal feeders and AMLs without extrarenal feeders, continuous variables were compared by using the independent t-test or the Wilcoxon rank-sum test, and categorical variables were compared with the chi-square test or Fisher's exact test. Simple logistic regression was performed by using the presence of extrarenal feeders as a binary categorical dependent variable (value, yes or no) and the largest tumor diameter and tumor volume as continuous independent variables. To compare the largest diameter and volume values for predicting the presence of extrarenal feeders, receiver operator characteristic (ROC) analyses were performed,

and the areas under the ROC curves (AUC) were compared. *P* values less than 0.05 (2-sided) were considered to be statistically significant. Statistical analyses were performed with PASW Statistics for Windows version 18.0 (SPSS Inc.) and MedCalc Statistical Software version 13.0 (MedCalc Software bvba).

## **Results**

For all 58 AMLs, the median value of the pre-embolization largest diameter was 8.4 cm (interquartile range, 6.3–10.5 cm), and the median value of the pre-embolization tumor volume was 136 mL (interquartile range, 49–277 mL); 29% (17 of 58) tumors had extrarenal arteries and 71% (41 of 58) did not.

The tumor characteristics for the AMLs are shown in Table 1. There were no significant differences between the groups with and without extrarenal feeders in terms of patient age, time interval between pre-embolization CT and TAE, the presence of concomitant disease (TSC or sLAM), tumor side, or tumor location. AMLs with extrarenal feeders were significantly larger than those without extrarenal feeders in terms of both volume (median value, 368 mL versus 109 mL,  $p < 0.0002$ ) and largest diameter (mean value, 12.0 cm versus 7.7 cm,  $p < 0.0001$ ).

Simple logistic regression also showed that the probability of having extrarenal feeders was significantly associated with largest tumor diameter and tumor volume; the probability of having extrarenal feeders increased as the tumor grew regardless of the largest tumor diameter (odds ratio per cm, 1.597 [95% CI, 1.241–2.053];  $p < 0.001$ ) or tumor volume (odds ratio per mL, 1.008 [95% CI, 1.003–1.013];  $p = 0.001$ ).

ROC analyses (Figure 3) showed that the AUC for the largest diameter was 0.83 (95% CI, 0.71–0.95) and the AUC for volume was 0.82 (95% CI, 0.70–0.95); the

difference in these AUCs did not reach statistical significance ( $p = 0.673$ ), indicating that these two indicators have similar predictive values. Using Youden's J statistic, the optimal values for tumor volume and largest tumor diameter were 266 mL and 10.5 cm, respectively. Those two values had the same sensitivity and specificity of 65% and 93%, respectively, for predicting the presence of extrarenal feeders. In addition, we found that a largest diameter of  $>6.5$  cm had a sensitivity and specificity of 100% and 41%, respectively.

From the results of the ROC analyses and Youden's J statistic analyses, all tumors could be divided into three groups on the basis of largest diameter: AMLs  $\leq 6.5$  cm ( $n = 16$ ), AMLs 6.6–10.5 cm ( $n = 28$ ), and AMLs  $>10.5$  cm ( $n = 14$ ). Tumor characteristics for each of the three groups are shown in Table 2. For AMLs  $>10.5$  cm, the frequency of extrarenal feeders was 79% (11/14), which was much higher than that for AMLs  $\leq 6.5$  cm (0% [0/16]) and that for AMLs 6.6–10.5 cm (21% [6/28]) ( $p < 0.001$ , respectively). Although the frequency of extrarenal feeders among AMLs 6.6–10.5 cm was higher than that among AMLs  $\leq 6.5$  cm, the difference was not statistically significant ( $p = 0.072$ ).

## **Discussion**

This retrospective study aimed to investigate factors associated with the presence of extrarenal feeders to renal AMLs. There were no significant differences between AMLs with and without extrarenal feeders in terms of patient age, tumor location, and the presence of concomitant disease, indicating that these factors are not significantly associated with the presence of extrarenal feeders. Large tumor size, however, was a significant factor, and simple logistic regression showed that the probability of extrarenal feeders increased with both largest tumor diameter and tumor volume.

Simple logistic regression was used rather than a multivariable model because only tumor size was significant in our initial comparisons (Table 1). Largest tumor diameter and tumor volume predicted the presence of extrarenal feeders with similarly high discrimination abilities in ROC analyses. Both largest diameter and volume have the advantage of being objective and quantitative, although the measurement of largest diameter is easier and quicker and does not require the use of volume calculation software. Therefore, from a clinical application perspective, largest diameter may be preferred over volume as an indicator.

In this study, the determination of renal AMLs with or without extrarenal feeders was performed by using a combination of arteriography obtained during TAE and CTA obtained before and after TAE. Renal arteriography, which was available for each patient, was used to decide whether the feeders of RB origin were extrarenal. Anatomically, the inferior adrenal artery and the capsular artery usually originate from the renal artery or one of its branches [24]. When these arteries feed renal AMLs, they are termed RB-origin extrarenal feeders in this research, but they may be confused with intrarenal feeders that supply both the renal parenchyma and the target tumors. Non-contribution to the renal parenchyma on renal arteriography is a useful sign to differentiate RB-origin extrarenal feeders from intrarenal feeders. CTA is a valuable tool for depicting the vascular anatomy in a variety of anatomical regions [25]. With excellent spatial resolution and rapid acquisition, CTA can be used clinically to evaluate vessels as small as 1 mm in diameter and has been applied to imaging of the coronary, renal, cerebral, and pulmonary systems [25, 26]. Further, compared to conventional abdominal aortography, CTA does not have the weakness of vessels overlapping on the monitor, which may cause potential extrarenal feeders of AB origin to be obscured by abundant normal abdominal vessels [20]. Therefore,

pre-embolization CTA is used routinely in our department to detect the parasitic vascularization of target AMLs before TAE and was used to detect extrarenal feeders of AB origin in the present study.

Angiogenic components of renal AMLs are made up of irregular, aneurismal, and tortuous blood vessels that are supplied by the feeding arteries [27]. Although benign, renal AMLs have the potential to grow substantially [11]. As an AML enlarges, the blood flow entering the tumor increases, and the arteries that feed the renal AML usually become more numerous and complex, potentially presenting as extrarenal feeders. Previous studies have reported that the renal capsular artery, the intercostal artery, the lumbar artery, the adrenal artery, the inferior phrenic artery, the ureteral artery, and the gonadal artery can supply renal AMLs [28-32]. However, these studies were mostly case reports or descriptions of individual cases within original articles, and there is a paucity of reports investigating predictors of the presence of extrarenal feeders. In contrast, with the inclusion of consecutive subjects and the use of statistical analyses, our study was designed to investigate predictive factors for the presence of extrarenal feeders.

Non-occlusion or incomplete occlusion of extrarenal feeders to renal AML can lead to recurrence of the target tumor and necessitate a repeat procedure such as surgery or TAE. The present study demonstrated that the probability of having extrarenal feeders increased as tumor size enlarged and was as high as 79% in AMLs >10.5 cm in largest diameter. Therefore, we suggest that for AMLs >10.5 cm, it is mandatory to address extrarenal feeders in order to avoid recurrence after embolotherapy. Conversely, because this study demonstrated that a largest tumor diameter of >6.5 cm has a 100% sensitivity for predicting the presence of extrarenal feeders to renal AMLs, we suggest that the criterion of largest diameter  $\leq 6.5$  cm can

be used to exclude the presence of extrarenal feeders for renal AML cases. Therefore, for AMLs that require embolotherapy and for which the largest diameter is not >6.5 cm, procedures for detecting extrarenal feeders for embolotherapy can be avoided, which may help to reduce operation time.

Our research has some limitations. First and foremost, our study lacks a reference standard for the value of CTA in the detection of AB-origin feeders. As mentioned above, for the cases in this study, pre-TAE CTA rather than aortography was used to detect AB-origin feeders mainly to avoid having abdominal vessels overlap on the monitor, a disadvantage with conventional aortography. However, the lack of aortography may mean that some potential CTA-negative AB feeders went undetected, which may result in false-negative cases in the group without extrarenal feeders. In our opinion, the best method to determine the presence or absence of AB-origin feeders is to perform selective catheter angiography of aortic branches, but that is impossible to do in a retrospective study. However, in our study, for tumors in the group without extrarenal feeders, the post-TAE CTA was used to control for the absence of AB-origin extrarenal feeders, and for those in the group with extrarenal feeders, the presence of AB-origin extrarenal feeders was confirmed by catheter angiography during the TAE procedure. Second, because our study is retrospective and involved a single center, the accuracy of our data may be affected by reporting bias [33]. Third, because the sample size for the group of AMLs with extrarenal feeders was small, the factors associated with the type of extrarenal feeders were not investigated in the present study. In the future, as more cases accumulate, a further study to investigate the factors linked to the types of extrarenal feeders should be performed.

## **Conclusion**

The presence of extrarenal feeders to renal AMLs is associated with large tumor size, but not with patient age, concomitant disease (TSC or sLAM), or tumor location.

AMLs >10.5 cm have a high frequency (79%) of extrarenal feeders, making it mandatory to search for feeders to them in order to avoid incomplete embolization; AMLs  $\leq$ 6.5 cm do not have extrarenal feeders, making the search for these feeders unnecessary.

## **References**

1. Avila NA, Dwyer AJ, Moss J (2017) Active surveillance of nonfatty renal masses in patients with lymphangioleiomyomatosis: use of CT features and patterns of growth to differentiate angiomyolipoma from renal cancer. *AJR Am J Roentgenol* 209:611-619.
2. Krishnan A, Kaza RK, Vummidi DR (2016) Cross-sectional imaging review of tuberous sclerosis. *Radiol Clin North Am* 54:423-440.
3. Flum AS, Hamoui N, Said MA, et al (2016) Update on the diagnosis and management of renal angiomyolipoma. *J Urol* 195:834-846.
4. Umeoka S, Koyama T, Miki Y, Akai M, Tsutsui K, Togashi K (2008) Pictorial review of tuberous sclerosis in various organs. *Radiographics* 28:e32.
5. Baron Y, Barkovich AJ (1999) MR imaging of tuberous sclerosis in neonates and young infants. *AJNR Am J Neuroradiol* 20:907-916.
6. Van Baal JG, Smits NJ, Keeman JN, Lindhout D, Verhoef S (1994) The evolution of renal angiomyolipomas in patients with tuberous sclerosis. *J Urol* 152:35-38.

7. Yeoh ZW, Navaratnam V, Bhatt R, McCafferty I, Hubbard RB, Johnson SR (2014) Natural history of angiomyolipoma in lymphangioleiomyomatosis: implications for screening and surveillance. *Orphanet J Rare Dis* 9:151.
8. Harknett EC, Chang WY, Byrnes S, et al (2011) Use of variability in national and regional data to estimate the prevalence of lymphangioleiomyomatosis. *QJM* 104:971-979.
9. Bernstein SM, Newell JJ, Adamczyk D, Mortenson RL, King TJ, Lynch DA (1995) How common are renal angiomyolipomas in patients with pulmonary lymphangioleiomyomatosis? *Am J Respir Crit Care Med* 152:2138-2143.
10. Nelson CP, Sanda MG (2002) Contemporary diagnosis and management of renal angiomyolipoma. *J Urol* 168:1315-1325.
11. Kiefer RM, Stavropoulos SW (2017) The role of interventional radiology techniques in the management of renal angiomyolipomas. *Curr Urol Rep* 18:36.
12. Yamakado K, Tanaka N, Nakagawa T, Kobayashi S, Yanagawa M, Takeda K (2002) Renal angiomyolipoma: relationships between tumor size, aneurysm formation, and rupture. *Radiology* 225:78-82.
13. Oesterling JE, Fishman EK, Goldman SM, Marshall FF (1986) The management of renal angiomyolipoma. *J Urol* 135:1121-1124.
14. Ramon J, Rimon U, Garniek A, et al (2009) Renal angiomyolipoma: long-term results following selective arterial embolization. *Eur Urol* 55:1155-1161.
15. Kothary N, Soulen MC, Clark TW, et al (2005) Renal angiomyolipoma: long-term results after arterial embolization. *J Vasc Interv Radiol* 16:45-50.
16. Sivalingam S, Nakada SY (2013) Contemporary minimally invasive treatment options for renal angiomyolipomas. *Curr Urol Rep* 14:147-153.

17. Muller A, Rouviere O (2015) Renal artery embolization-indications, technical approaches and outcomes. *Nat Rev Nephrol* 11:288-301.
18. Hoshii T, Morita S, Ikeda Y, Hasegawa G, Nishiyama T (2017) Laparoscopic retroperitoneal nephron-sparing surgery without renal artery clamping with preoperative selective arterial embolization for management of right renal angiomyolipoma of diameter 10 cm: A Case Report. *J Endourol Case Rep* 3:13-16.
19. Cai T, Rozzanigo U, Tiscione D, Dalla PP, Malossini G (2011) Selective arterial embolization for renal angiomyolipoma treating: the role of pain. *Eur J Vasc Endovasc Surg* 41:134, 135.
20. Hiromura T, Nishioka T, Tomita K (2005) Spontaneous rupture of renal angiomyolipoma: value of multidetector CT angiography for interventional therapy. *Emerg Radiol* 12:53-54.
21. Ramaswamy RS, Darcy MD (2016) Arterial embolization for the treatment of renal masses and traumatic renal injuries. *Tech Vasc Interv Radiol* 19:203-210.
22. Northrup H, Krueger DA (2013) Tuberous sclerosis complex diagnostic criteria update: recommendations of the 2012 International Tuberous Sclerosis Complex Consensus Conference. *Pediatr Neurol* 49:243-254.
23. Johnson SR, Cordier JF, Lazor R, et al (2010) European Respiratory Society guidelines for the diagnosis and management of lymphangiomyomatosis. *Eur Respir J* 35:14-26.
24. Bordei P, St AD, Sapte E, Iliescu D (2003) Morphological aspects of the inferior suprarenal artery. *Surg Radiol Anat* 25:247-251.
25. Dewhurst C, O'Neill S, O'Regan K, Maher M (2012) Demonstration of the course of the posterior intercostal artery on CT angiography: relevance to interventional radiology procedures in the chest. *Diagn Interv Radiol* 18:221-224.

26. Choi S, Trieu J, Ridley L (2010) Radiological review of intercostal artery: anatomical considerations when performing procedures via intercostal space. *J Med Imaging Radiat Oncol* 54:302-306.
27. Rimon U, Duvdevani M, Garniek A, et al (2006) Large renal angiomyolipomas: digital subtraction angiographic grading and presentation with bleeding. *Clin Radiol* 61:520-526.
28. Rimon U, Duvdevani M, Garniek A, et al (2006) Ethanol and polyvinyl alcohol mixture for transcatheter embolization of renal angiomyolipoma. *AJR Am J Roentgenol* 187:762-768.
29. Ashebu SD, Dahniya MH, Elshebiny YH, Varro J, Al-Khawari H (2002) Giant bleeding renal angiomyolipoma: diagnosis and management. *Australas Radiol* 46:115-118.
30. Stamatiou KN, Moschouris H, Marmaridou K, Kiltenis M, Kladis-Kalentzis K, Malagari K (2016) Combination of superselective arterial embolization and radiofrequency ablation for the treatment of a giant renal angiomyolipoma complicated with caval thrombus. *Case Rep Oncol Med*. DOI: 10.1155/2016/8087232.
31. Incedayi M, Turba UC, Arslan B, et al (2010) Endovascular therapy for patients with renal angiomyolipoma presenting with retroperitoneal haemorrhage. *Eur J Vasc Endovasc Surg* 39:739-744.
32. Kato H, Kuwatsuru R, Inoue T, Okada S, Aida M, Yamashiro Y (2018) Superselective transcatheter arterial embolization for large unruptured renal angiomyolipoma in lymphangioliomyomatosis. *J Vasc Interv Radiol* 29:958-965.
33. Sheth RA, Feldman AS, Paul E, Thiele EA, Walker TG (2016) Sporadic versus tuberous sclerosis complex-associated angiomyolipomas: predictors for long-term outcomes following transcatheter embolization. *J Vasc Interv Radiol* 27:1542-1549.

## **Table and Figure legends**

**Table 1** Characteristics of all renal AMLs and comparison of characteristics between renal AMLs with and without extrarenal feeders.

**Table 2** Characteristics of AMLs  $\leq 6.5$  cm, 6.6–10.5 cm, and  $>10.5$  cm.

**Figure 1** A 52-year-old woman with tuberous sclerosis complex. (A) Pre-embolization axial CT image shows a fat-containing angiomyolipoma (white arrows) at the lower pole of the left kidney. (B) Pre-embolization 3-dimensional CT angiography shows that the left ureteral artery (white arrow) and a branch (white triangle) of the inferior mesenteric artery (IMA) are feeding arteries of the target tumor. The left ureteral artery (C, black arrow) and the branch of the IMA (D, black triangle) were confirmed to be feeding arteries by superselective angiography obtained during embolization.

**Figure 2** A 55-year-old woman with tuberous sclerosis complex. (A) Coronal multiplanar reconstruction (MPR) image of pre-embolization CT shows a fat-containing angiomyolipoma (long white arrows) located at the upper pole of the right kidney. (B) Renal arteriography shows that the extrarenal feeder of the superior capsular artery (black arrow) is feeding the target tumor and multiple intratumoral aneurysms (short white arrows) are fed by intrarenal branches of the renal artery.

**Figure 3** Receiver operator characteristics curves for largest tumor diameter and tumor volume for predicting the presence of extrarenal feeders to renal angiomyolipomas.

**Table 1 Characteristics of all renal AMLs and comparison of characteristics between renal AMLs with and without extrarenal feeders**

	All AMLs (n=58)	AMLs with extrarenal feeders (n = 17)	AMLs without extrarenal feeders (n = 41)	P-value (statistical test)
Mean patient age, years ( $\pm$ SD)	40 ( $\pm$ 12)	40 ( $\pm$ 11)	37 ( $\pm$ 12)	0.337 (independent t-test) NS
Median interval between pre-embolization CT and TAE, days (interquartile range)	51 (30-79)	54 (27-86)	43 (31-80)	0.797 (Wilcoxon rank sum test) NS
Coexistent TSC/sLAM (n = number of AMLs)				0.435 (Fisher's exact test) NS
TSC	26	9	17	
sLAM	22	7	15	
None	10	1	9	
Median tumor volume, mL (interquartile range)	136 (49-277)	368 (119-607)	109 (44-192)	<0.0002 (Wilcoxon rank sum test)
Median (interquartile range) or mean ( $\pm$ SD) largest diameter, cm	8.4 (6.3-10.5)	12.0 ( $\pm$ 3.7)	7.7 ( $\pm$ 2.3)	<0.0001 (Wilcoxon rank sum test)
Tumor side (n = number of AMLs)				0.773 (chi-square test) NS
Left side	29	9	20	
Right side	29	8	21	
Tumor location (n = number of AMLs)				0.147 (chi-square test) NS
Upper pole	17	8	9	
Middle portion	21	4	17	
Lower pole	20	5	15	

AML, angiomyolipoma; sLAM, sporadic lymphangioliomyomatosis; NS, not significant; SD, standard deviation; TAE, transcatheter arterial embolization; TSC, tuberous sclerosis complex

**Table 2 Characteristics of AMLs  $\leq 6.5$  cm, 6.6–10.5 cm, and  $>10.5$  cm**

	AMLs $\leq 6.5$ cm (n = 16)	AMLs 6.6–10.5 cm (n = 28)	AMLs $>10.5$ cm (n=14)
Mean patient age, years ( $\pm$ SD)	36 ( $\pm 12$ )	37 ( $\pm 11$ )	39 ( $\pm 12$ )
Coexistent TSC/sLAM (n = number of AMLs)			
TSC	3	14	9
sLAM	9	9	4
None	4	5	1
Median value of largest diameter, cm (interquartile range)	5.5 (4.9-6.0)	8.6 (7.6-9.3)	14.1 (12.9-15.2)
Median value of tumor volume, mL (interquartile range)	38 (33-46)	141 (94-200)	466 (319-610)
Tumor side (n = number of AMLs)			
Left side	5	18	6
Right side	11	10	8
Tumor location (n = number of AMLs)			
Upper pole	6	5	6
Middle portion	4	14	3
Lower pole	6	9	5
Tumors with extrarenal feeders, N (Frequency)	0 (0/16, 0%)	6 (6/28, 21%)	11 (11/14, 79%)
Extrarenal feeders (n = number of feeder)			
RB-origin	0	7	16
AB-origin	0	0	10
	0	0	6

AML, angiomyolipoma; AB, aortic branches; RB, renal arterial branches; sLAM, sporadic lymphangioliomyomatosis; SD, standard deviation; TSC, tuberous sclerosis complex

Figure 1

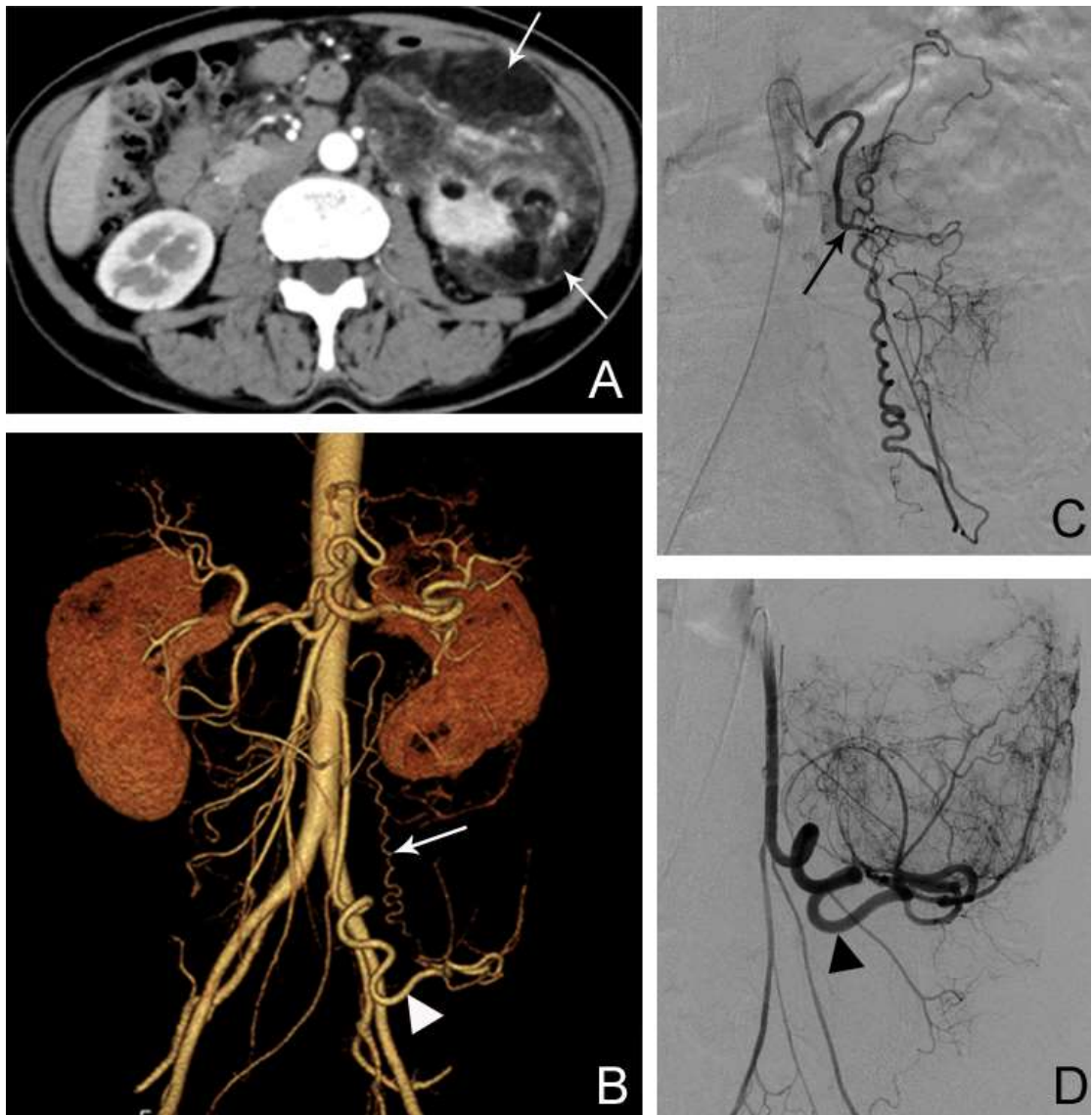


**Figure 2**

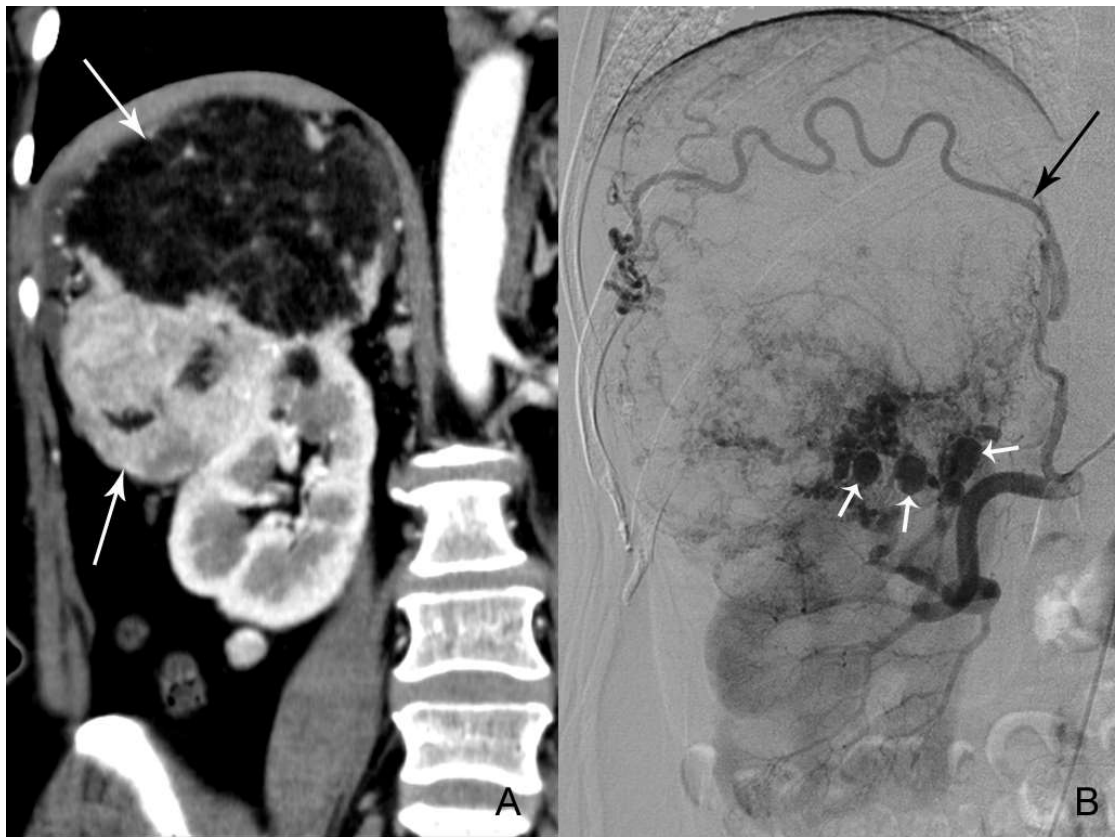


Figure 3

